

## Ultrafast Coherent Control and Destruction of Excitons in Quantum Wells

A. P. Heberle and J. J. Baumberg

*Hitachi Cambridge Laboratory, Madingley Road, Cambridge CB3 0HE, United Kingdom*

K. Köhler

*Fraunhofer-Institut für Angewandte Festkörperphysik, 79108 Freiburg, Germany*

(Received 5 May 1995)

We demonstrate the coherent destruction of photogenerated excitons in semiconductor quantum wells within a few hundred femtoseconds of their excitation. Coherent control of carrier dynamics is achieved with phase-locked pairs of 100 fs infrared pulses. The technique induces an optical response which is faster than the inverse of the exciton linewidth superseding Fourier limits for a single pulse. Energy selectivity enables the coherent transfer of angular momentum between hole states. Such phase-tailored pulse trains can be utilized to investigate the generation process and intermediate virtual states in quantum structures.

PACS numbers: 78.47.+p, 42.50.Md, 71.35.+z, 73.20.Dx

The ultimate control of a quantum mechanical system with light depends not only on the system amplitude but also on its phase. The effect of a sequence of light pulses on an optical transition varies strongly with their relative phase if the excited system stays coherent for a sufficiently long time. This coherent control of quantum dynamics has been pursued with great enthusiasm to direct photochemical reactions down a particular pathway [1,2]. Although such chemical manipulation is still in its infancy, a variety of coherent phenomena have been elicited from the interaction of phase-locked optical pulse sequences with atomic and molecular species [3–6]. These experiments revealed oscillations in the time-integrated fluorescence when the relative phase between the exciting pulses was changed. In semiconductors, coherent control was proposed to induce photocurrents [7], but picosecond phase-relaxation times in solids require only recently developed ultrafast laser sources for the investigation of coherent phenomena [8–10]. Initial coherent control experiments in semiconductors have investigated the manipulation of THz radiation from coupled quantum wells (QW's) and demonstrated the astonishing optical down-mixing produced by interfering oscillating electronic wave packets [11,12]. Of even greater interest is the manipulation of carrier *populations*, because it promises to remove some of the main obstacles to ultrafast optoelectronics and all-optical switching which are degraded by long-lived carrier dwell times in the active regions. However, complete coherent control requires long phase-relaxation times, and it is not self-evident that the associated narrow linewidths permit a fast system response. To our knowledge, the phase engineering of carrier populations on femtosecond time scales has never been reported.

Here, we demonstrate the ultrafast dynamics of optical transitions at rates far in excess of their spectral linewidths by using coherent carrier control (CCC). A sequence of two optical pulses with well defined phase correlation first

creates excitons within a semiconductor quantum well and then removes them again by destructive interference. In contrast to previous experiments, we directly time-resolve the carrier dynamics and demonstrate that CCC is not limited by the transition linewidth. Coherent control thus enables optical nonlinearities to be directly switched on and off within a few hundred femtoseconds. The phase-locked pulse sequences let us examine transient “virtual” states by tailoring the time dependence of the excitation spectrum. Irreversible optical absorption is tracked as the excitons lose their coherence. The energy selectivity of CCC allows us to demonstrate phase-dependent transfer of angular momentum between photoexcited heavy-hole (hh) and light-hole (lh) excitons.

Figure 1(a) shows the setup which uses a mode-locked Ti:sapphire laser as the source of transform-limited pulses. An actively stabilized Michelson interferometer in the pump beam produces two phase-locked pulses of temporal separation  $\tau_{12}$ . Figure 1(b) shows the spectral content of the pulse pair when separated by 10 times their pulse width. The high contrast ( $>50 : 1$ ) interference fringes show maxima at  $n\lambda = c\tau_{12}$  ( $n$  integer) which stay fixed for any duration and demonstrate the excellent phase stability ( $\lambda/100$ ) of the arrangement. Translation by  $\lambda/2$  ( $\Delta\tau_{12} = 1.34$  fs) reverses the fringe pattern. The pump-induced reflectivity change ( $\Delta R$ ) and the diffracted four-wave-mixing (FWM) signal, sampled at the probe delay time  $\tau_x$ , access both population and polarization components of the interband transition. The pump and probe beams are polarized perpendicularly for  $\Delta R$  and parallel for FWM experiments and have comparable intensities, each pulse exciting exciton densities of  $\sim 10^{10}$  cm $^{-2}$ . All measurements were performed at a temperature of 4 K.

The sample contains five 12 nm GaAs QW's separated by 12 nm Al $_{0.3}$ Ga $_{0.7}$ As barriers. Reflectivity and photoluminescence data in Fig. 2(a) resolve a 0.7 meV linewidth of the lowest hh exciton transition. The reflection geome-

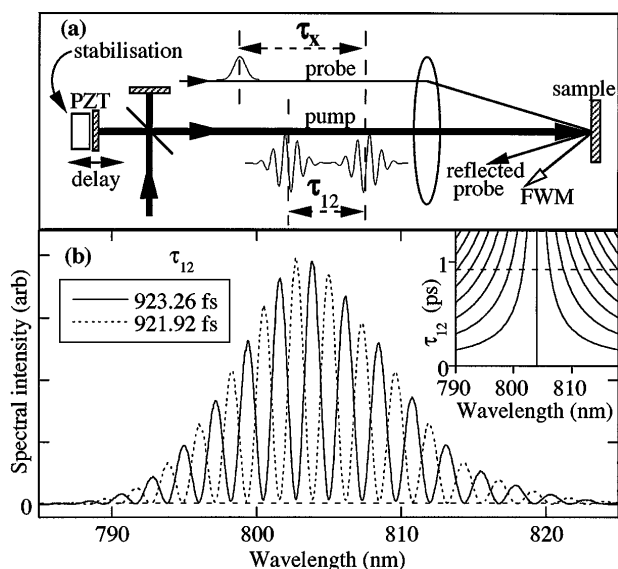


FIG. 1. (a) Experimental setup. (b) Spectrum of the pump pulse sequence showing the reversal of interference at times separated by  $\lambda_{\text{laser}}/2c$ . Inset: calculated fringe peak positions vs  $\tau_{12}$  for separations yielding constructive interference at the central wavelength  $\lambda_{\text{laser}}$ .

try avoids strain problems which are inevitable in samples etched for transmission experiments. The laser was tuned to the hh exciton energy, and a pulse width of 150 fs was used to reduce excitation of excess free carriers which decrease the phase-relaxation time. The results reported in this paper do not depend on these special QW's and are also observed on different samples with sufficiently narrow linewidths.

Figure 2(b) demonstrates coherent control of the exciton density. The diagrams display the interferogram of the pump-induced reflectivity change  $\Delta R$  (solid) and the pump intensity (dashed) versus  $\tau_{12}$ . The probe pulse records  $\Delta R$  and therefore the resulting exciton density after a delay of  $\tau_x = 10$  ps when the excitons have lost their phase coherence. The insets detail portions of the several-thousand interference fringes, shown with sinusoidal fits through the data points, while the lower plot records their amplitude. The exciton population oscillates with a period  $T_{\text{hh}} = h/E_{\text{hh}}$  corresponding to the lowest hh exciton energy  $E_{\text{hh}}$ . These oscillations result from the interference between coherent excitons surviving from the first pulse, with the second pulse and yield frequency, phase, and amplitude dynamics as a function of time delay. The decay of the oscillations shows the decay of the coherent exciton population created by the first pulse. The weak quantum beats modulating the envelope agree well with the observed energy separation of the lh and hh excitons ( $\tau_{\text{hl}} = h/E_{\text{hl}}$ ). The simultaneously recorded interference of the pump pulses demonstrates that their phase difference strongly influences the eventual carrier population long after there is negligible temporal overlap.

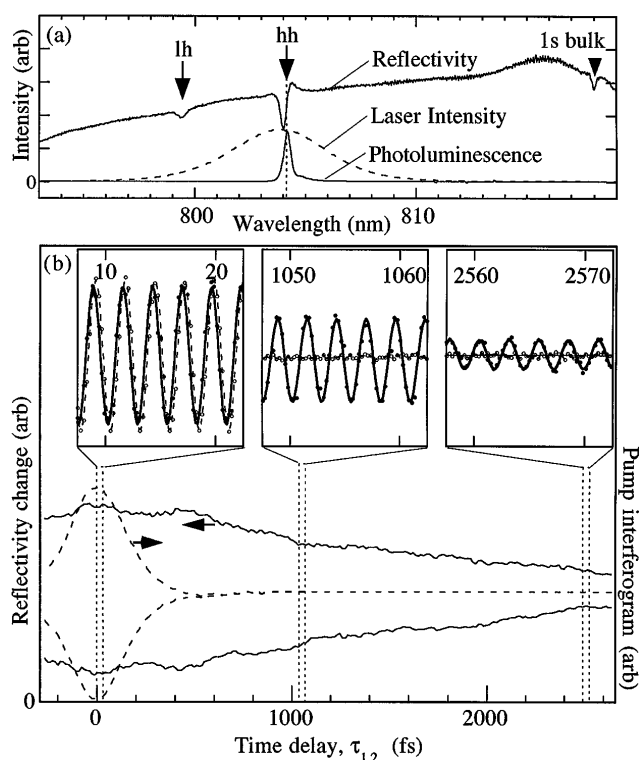


FIG. 2. (a) Reflectivity and photoluminescence of  $5 \times 12$  nm GaAs QW sample at 4 K. Dashed: spectrum of 150 fs pump pulse. (b) Maximum and minimum pump-induced reflectivity changes at  $\tau_x = 10$  ps (solid) and pump pulse interferogram (dashed) vs  $\tau_{12}$ . Insets: expanded interference oscillations with sinusoidal fits through the data points.

The interference oscillations have a simple origin in the spectral domain. The troughs (or peaks) in the spectrum of the pump pulse pair in Fig. 1(b) are positioned on top of the exciton line for destructive (or constructive) interference. Increasing  $\tau_{12}$  narrows the spectral fringes [Fig. 1(b) inset], which unavoidably excite more of the exciton line and thus limit the carrier destruction. This picture suggests that the exciton responds only to the spectral band with which it overlaps, implying a slow response limited by the inverse linewidth. However, we will show that this cannot be the case and additional off-resonant excitation creates an ultrafast response. The phase-locked pump pulse sequence is equivalent to a longer pulse whose center portion has been excised, allowing us to investigate intermediate virtual carriers. The pump spectrum is smooth [Fig. 2(a)] until the second pump pulse arrives, and excitons are excited; however, afterwards the spectrum develops interference fringes [Fig. 1(b)]. In case of destructive interference, there are no longer any photons at the exciton energy and the intermediate exciton population is reextracted. Such an excess spectral distribution at the beginning of a pulse has recently been suggested to enhance ultrafast carrier scattering in semiconductors, because Heisenberg's principle broadens the

initial spectral content of a transform limited laser pulse above the spectral width of the full pulse [13–15]. Although no direct verification of this effect was previously possible, our pump pulse sequence directly resolves the nature of these intermediate virtual states.

The time-resolved evolution of the population a fixed  $\tau_{12}$  demonstrates that a large intermediate exciton population is excited. Figure 3(a) presents such evidence in  $\Delta R(\tau_x)$  for  $\tau_{12}$  of 402.00 and 403.34 fs, equivalent to 150.00 and 150.50  $T_{hh}$ . The dotted curves show the effect of each pump pulse alone, with the latter pulse set to excite a smaller carrier density than the first. The solid line (150.50  $T_{hh}$ ) resolves the creation of an initial exciton population followed by its subsequent destruction within a few hundred femtoseconds. The resulting exciton density collapses below that for either pump pulse alone unambiguously verifying coherent destruction. In the opposite extreme, if the second laser pulse arrives 150.00  $T_{hh}$  later

(dashed), *more* carriers are generated than from the sum of the two pump pulses individually. The in-phase carriers that are already excited increase the subsequent probability of absorption if they remain coherent. As the time delay between the pump pulses increases, more phase scattering has occurred and destruction is lost [Figs. 3(a) and 3(b)].

The optical Bloch equations describe the observed femtosecond exciton evolution [16]. Figure 3(d) shows the graphical interpretation of the Bloch vector  $\mathbf{B}$  in which the population  $N = 1 + B_z$  and the interband polarization  $P = B_x + iB_y$ , where  $\Delta R \propto N$  [17]. The hh exciton dipole moment  $\mu$  couples to optical pulses with envelope  $E(t)$  tuned on-resonance. The first pulse rotates the vector by  $\theta_1$  out of the ground state leading to an exciton density  $N_1 \propto 1 - \cos\theta_1$ , where  $\hbar\theta_1 = \mu \int E_1(t) dt$ . We assume that carrier recombination is minimal and neglect inhomogeneous broadening, which is small for this sample. Thus the carrier density remains unchanged for the interval between the pulses, but the associated interband polarization decays by a factor  $\eta = \exp(-\tau_{12}/T_2)$  for a dephasing time of  $T_2$ . The second pulse provokes a further rotation  $\theta_2 = (\mu/\hbar) \int E_2(t) dt$  of the Bloch vector either returning it back towards the initial state or exciting more carriers, according to the relative phase between the pulses. The resultant maximum and minimum carrier densities are

$$N_{\pm} = 1 - \cos(\theta_1 \pm \theta_2) \pm (\eta - 1) \sin\theta_1 \sin\theta_2. \quad (1)$$

For weakly excited systems, this yields  $N_{\pm} = (\theta_1^2 + \theta_2^2)/2 \pm \eta\theta_1\theta_2$ , so that the phase-dependent  $\Delta R$  contribution decays with a lifetime of  $T_2$ . Phase scattering implies that greater destruction is achieved if the second pulse is attenuated ( $\theta_2 = \eta\theta_1$ ), matching it to the remaining coherent exciton population to avoid overshooting the minimum density. Figure 3(b) exhibits nonoptimal destruction and overshoot at  $\tau_{12} = 300.50 T_{hh} = 805.34$  fs, which is improved using a relative amplitude of 1.6 : 1 for  $\langle E_1 \rangle : \langle E_2 \rangle$  as shown in Fig. 3(c). Our experiments contrast with recent measurements of Rabi flopping in semiconductors [9] in which the system is “overdriven” by a high-intensity pulse, reaching a maximally excited exciton population before deexciting. In the present case, the pump pulse sequence remains within a perturbative response of the exciton, avoiding the saturated exciton densities at which carrier-carrier scattering dominates the dynamics, and permitting destructive interference at lower densities.

The coherent polarization of excitons can be coherently controlled as well as their density. Figures 4(a) and 4(b) show simultaneously manipulated FWM which exhibits complete destruction when the pump pulses are arranged optimally. While  $\Delta R$  measures the total exciton population, FWM isolates solely the coherent exciton polarization and can always be demolished. The destruction

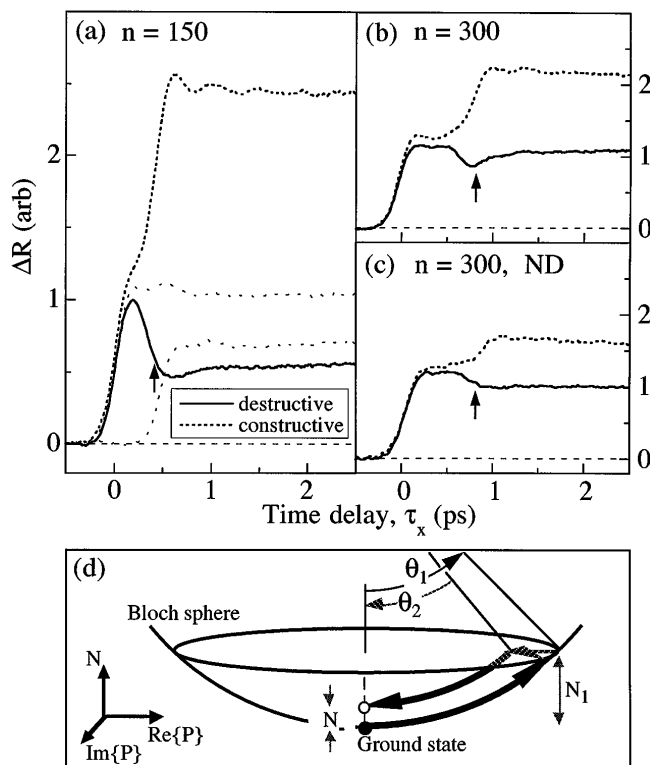


FIG. 3. (a)–(c) Time-resolved enhancement (dashed,  $\tau_{12} = nT_{hh}$ ) and destruction [solid,  $\tau_{12} = (n + \frac{1}{2})T_{hh}$ ] of the pump-induced reflection change. The arrows indicate the arrival of the second pump pulse. The dotted lines in (a) record the effects of each pump pulse alone. The second pump beam is attenuated by 60% with an ND filter in (c). Long-lived residual signals ( $\sim 10\%$ ) originating from incomplete carrier relaxation are removed from the data. (d) The effect of the pump pulses on the initially unexcited Bloch vector,  $\mathbf{B} = (0, 0, -1)$ . Pulse 1 rotates  $\mathbf{B}$  by  $\theta_1$  creating a population  $N_1$ . The concomitant polarization decays as carriers are scattered, before the destructively phased pulse 2 rotates  $\mathbf{B}$  back by  $\theta_2$  leaving  $N_-$  excited excitons behind.

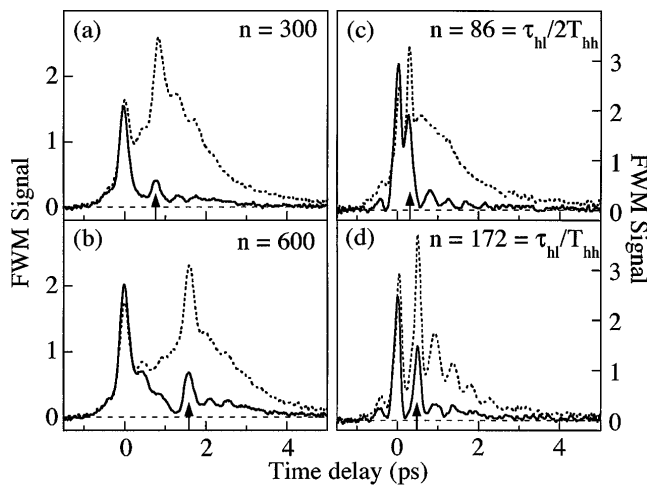


FIG. 4. Four-wave-mixing intensity at selected pump pulse separations showing constructive (dashed,  $\tau_{12} = nT_{hh}$ ) and destructive [solid,  $\tau_{12} = (n + \frac{1}{2})T_{hh}$ ] interference. The laser pulse width is 150 fs in (a) and (b) and 65 fs in (c) and (d). Pronounced beating is seen in (d) after one hh-lh beat period which is eliminated if only half this period has elapsed (c).

significantly overshoots at  $600 T_{hh}$  [Fig. 4(b)], and the resulting reversal of the polarization direction is visible as a minimum around 1.25 ps, after which the phase of the signal inverts. The comparison between FWM and  $\Delta R$  shows markedly the effect of incoherence on the potential for complete destruction. In spite of extensive experiments at a range of exciton densities, polarizations, and confinements, we have been unable to achieve destruction greater than 70% of the initial carrier density in the  $\Delta R$  experiments. It is currently unclear whether this incomplete destruction indeed implies a very fast phase scattering contribution of free carriers generated at the very beginning of the first pump pulse or whether it is connected to the fact that the excitons are not ideal two-level atoms. Initial fast phase scattering would pass undetected in a FWM experiment.

The spectral dependence of the interference [Fig. 1(b)] implies that coherent control is highly energy selective and can be tuned to simultaneously manipulate several species in different ways. As an example, hh excitons experience constructive and simultaneously lh excitons destructive interference when the hh exciton line coincides with a peak and the lh exciton line with a trough of the pump spectrum. The laser was optimized for shortest pulse widths (65 fs), to excite both hh and lh exciton states. After one beat period  $\tau_{12} = \tau_{hh} = 172T_{hh}$ , the hh and lh excitons have the same phase and can both be selectively enhanced or destroyed by the second pump pulse

[Fig. 4(d)]. The pronounced beating seen in the constructive FWM signal implies that the lh excitons have not phase scattered despite their degeneracy with the hh continuum. Figure 4(c) is taken with  $\tau_{12} = \tau_{hh}/2 = 86 T_{hh}$  so that the phases of the hh and lh excitons differ by  $\pi$ . In this case interference destroys either exciton variety while enhancing the remaining population. The second pump pulse interconverts hh and lh excitons, hence FWM shows the remaining hole population [18]. The absence of quantum beats in the dashed curve of Fig. 4(c) attests to this result. The interconversion employs photons to transfer angular momentum between the hh ( $m_j = \pm 3/2$ ) and lh ( $m_j = \pm 1/2$ ) states. Coherent control allows the isolation of target excitations of interest while retaining time resolution hard to match using other techniques.

In summary, phase-locked femtosecond pulses enable ultrafast coherent carrier control in quantum structures. Destruction of excitons is possible on time scales much faster than the phase-relaxation time and can thus generate resonant but ultrafast nonlinear optical interactions. Such techniques have general applicability in a wide range of materials and yield novel excitation conditions that discern ultrafast processes at the onset of absorption.

- 
- [1] W.S. Warren, H. Rabitz, and M. Dahleh, *Science* **259**, 1581 (1993), and references therein.
  - [2] N.F. Scherer *et al.*, *J. Chem. Phys.* **95**, 1487 (1991).
  - [3] M.M. Salour and C. Cohen-Tannoudji, *Phys. Rev. Lett.* **38**, 757 (1977).
  - [4] F. Spano, M. Haner, and W.S. Warren, *Chem. Phys. Lett.* **135**, 97 (1987).
  - [5] J.T. Fourkas *et al.*, *J. Opt. Soc. Am. B* **6**, 1905 (1989).
  - [6] E. Tokunaga, A. Terasaki, and T. Kobayashi, *Opt. Lett.* **17**, 1131 (1992).
  - [7] G. Kurizki, M. Shapiro, and P. Brumer, *Phys. Rev. B* **39**, 3435 (1989).
  - [8] S. Weiss *et al.*, *Phys. Rev. Lett.* **69**, 2685 (1992).
  - [9] S.T. Cundiff *et al.*, *Phys. Rev. Lett.* **73**, 1178 (1994).
  - [10] See special issue, *Phys. Status Solidi (b)* **173** (1992), and references therein.
  - [11] P.C.M. Planken *et al.*, *Phys. Rev. B* **48**, 4903 (1993).
  - [12] I. Brener *et al.*, *J. Opt. Soc. Am. B* **11**, 2457 (1994).
  - [13] A.V. Kuznetsov, *Phys. Rev. B* **44**, 13 381 (1991).
  - [14] T. Kuhn and F. Rossi, *Phys. Rev. Lett.* **69**, 977 (1992).
  - [15] A. Leitenstorfer *et al.*, *Phys. Rev. Lett.* **73**, 1687 (1994).
  - [16] L. Allen and J.H. Eberly, *Optical Resonance and Two-Level Atoms* (Dover, New York, 1987).
  - [17] S. Schmitt-Rink, D.S. Chemla, and D.A.B. Miller, *Adv. Phys.* **38**, 89 (1989).
  - [18] The data are consistent with a hh:lh density of 6:1.